Measurements of a Persistent-Current Qubit Driven by an On-Chip Radiation Source

Jonathan L. Habif, Bhuwan Singh, Donald S. Crankshaw, and Terry P. Orlando

***Abstract*—Monolithic integration of control electronics with superconducting qubits will facilitate scalability of a superconducting quantum computer by reducing the room temperature electronics necessary for performing quantum state manipulation. We report the experimental results of the monolithic integration of an on-chip radiation source with a persistent-current (PC) qubit and dc SQUID measurement device. The devices were fabricated at MIT Lincoln Laboratory in a Nb/Al/AlOx/Nb trilayer process. The two PC qubit states were detected by measuring the switching current of an underdamped dc SQUID magnetometer inductively coupled to the qubit. The radiation source comprised an overdamped dc SQUID operating in the voltage state and inductively coupled to the qubit and measurement SQUID through a low-Q RLC filter. The oscillator was designed to have tunable amplitude and frequency to satisfy the requirements for coherent quantum manipulation of a superconducting PC qubit. We will discuss the measurements in the millikelvin regime and the effects of the oscillator noise on the state of the qubit.**

***Index Terms*—Quantum bits, quantum computing, qubit spectroscopy, SQUID oscillator.**

I. Introduction

SUPERCONDUCTING Josephson devices have been identified as attractive candidates for constructing a full-scale quantum computer [1]. Though atoms and molecules are more traditional quantum systems, under strict conditions the quantum mechanical properties of superconducting devices can be observed, engineered and exploited for the purpose of constructing a quantum coherent processor. Though quantum control in atomic systems is much more mature than that in superconducting systems, the fabrication capabilities of necessary to scale a quantum computer to a many-qubit architecture already exist in superconducting technology. Moreover, an extensive body of work exists on the development of superconducting analog and digital electronics which can be integrated monolithically with, and used for initialization, manipulation and readout of the qubits [2].

The state-of-the-art experiments with superconducting qubits have shown that a qubit can be fabricated such that it can be modeled as a two-level or many-level quantum system. Experimental progress thus far examining the quantum nature of these devices has included the spectroscopic probing of the energy level structure [3], coherent Rabi oscillations between energy levels corresponding to macroscopic degrees of freedom of the qubit, and spin-echo experiments where the wavefunction of a qubit is prepared and the phase of the constituent energy levels is followed during free Larmor oscillation [4]. In general, the entirety of these experiments involve a multitude of room temperature electronics in order to initialize, manipulate and readout the quantum state of the qubit. Function generators are used to modulate the magnetic field applied to the device. Microwave generators and gating electronics manipulate the qubit by supplying radiation pulses to the qubits, coherently driving population between energy levels of the system. Finally, function generators and voltage amplifiers are used to measure the qubit's final state. The equipment overhead for maintaining control of a single qubit is large, and the scalability to multi-qubit systems becomes a daunting endeavor. However, by capitalizing on the maturity of the superconducting integrated circuit foundries we can drastically reduce the amount of external electronics necessary to perform the manipulation and control of superconducting quantum coherent systems. In this experiment, we have replaced the laboratory microwave generator with a Josephson oscillator that is integrated monolithically with the superconducting flux qubit. The oscillator is a damped dc-SQUID that is inductively coupled to the flux qubit. When the dc-SQUID is driven to the voltage state it produces a microwave signal with a frequency spectrum that can be tuned by adjusting the supplied dc bias current. In this configuration the need for a microwave generator and high bandwidth signal line has been replaced with a dc current line and power source.

In this paper we characterize both the qubit and the dc-SQUID oscillator according to the fabricated parameters, and report on experimental measurements of the qubit operated with and without the accompaniment of a microwave signal from the oscillator. Data collected at 350 mK indicate both increased thermalization due to broad frequency noise coupled from the oscillator as well as signatures of stimulation between quantized energy levels of the system.

II. Circuit Characterization

The two discrete units of the complete circuit are the persistent-current (pc) qubit inductively coupled with a dc-SQUID magnetometer for readout of the qubit, and the highly damped dc-SQUID oscillator connected to a bandpass filter and inductively coupled to the pc-qubit. The entire circuit is shown schematically in Fig. 1.

Manuscript received October 4, 2004. This work was supported in part by the AFOSR Grant F49620-01-1-0457 under the DoD University Research Initiative on Nanotechnology (DURINT) program, and by the ARO student support Grant DAAD 19-01-1-0624.

The authors are with the Department of Electrical Engineering and Computer Science, Massachusetts Institute of Technology, Cambridge, MA 02139 USA (e-mail: jhabif@mit.edu).

Digital Object Identifier 10.1109/TASC.2005.850092

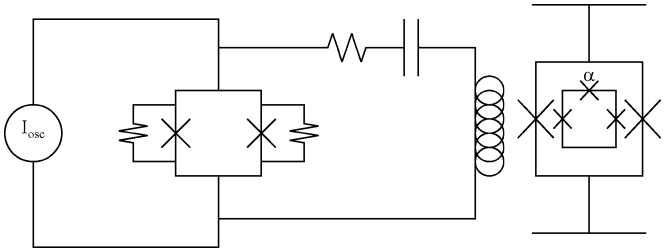

Fig. 1. A schematic representation of the on-chip oscillator circuit with a bandpass filter, coupled inductively to the pc-qubit and measurement SQUID. The entire circuit was fabricated monolithically in a superconducting foundry with $\mathrm{J_c} \sim 5.72\ \mu\mathrm{A}/\mu\mathrm{m}^2$.

A. Persistent-Current Qubit and Measurement SQUID

The design of the pc-qubit is crucial in engineering the quantum parameters of the system. The pc-qubit is a superconducting inductive loop, measuring 15 μm by 15 μm, broken by three Josephson junctions. Two of the junctions in the loop have critical current I_c while the third junction is smaller by value αI_c. When the pc-qubit is flux biased near one half flux quantum (Φ_0), the potential energy of the system is such that there is a stable minimum and a metastable minimum separated by an energy barrier. The height of the barrier in this double-well potential is determined by the factors α and I_c. By measuring the critical current of a larger Josephson junction on the same sample the critical current density (J_c) was determined to be 5.72 $\mu\mathrm{A}/\mu\mathrm{m}^2$. The area of the larger two junctions was designed to be 0.64 $\mu\mathrm{m}^2$, while the smaller junction was designed at 0.49 $\mu\mathrm{m}^2$. Effects in processing produce a "junction undercut", yielding smaller junctions than designed. It is possible to determine the fabricated size of the junctions by examining features of the qubit step that are due to energy level quantization in the device.

The underdamped dc-SQUID inductively coupled to the pc-qubit was designed with 1.0 $\mu\mathrm{m}^2$ Josephson junctions. The maximum critical current of the device was approximately 17 μA, indicating that the junctions were fabricated with an effective length of 1.2 μm per side. The SQUID is also shunted by 1 pF capacitors in order to shift the effective plasma frequency of the device away from the energy splitting of the qubit, thus detuning the channel for noise induced decoherence in the pc-qubit at this critical frequency.

Experiments were conducted on the pc-qubit by repeatedly measuring the critical current of the underdamped SQUID inductively coupled to the pc-qubit, while sweeping the magnetic flux applied to the qubit-SQUID system. When the flux applied to the pc-qubit is near $\Phi_0/2$ the potential energy landscape is that of a double well. Under optimal fabrication conditions, when the qubit is flux biased slightly above or below $\Phi_0/2$ there are energy levels in each well with localized probability amplitude. The magnetization of the pc-qubit enhances or cancels the flux bias of the dc-SQUID, thereby superimposing the qubit signal on the measured critical current of the dc-SQUID. When the flux supplied to the qubit is swept through $\Phi_0/2$ the current circulating in the qubit, and hence the qubit magnetization, undergo a transition as the energy of the qubit relaxes from one stable minimum to the other. This transition can be seen on the switching current measurement of the dc-SQUID and is referred to as the 'qubit step'.

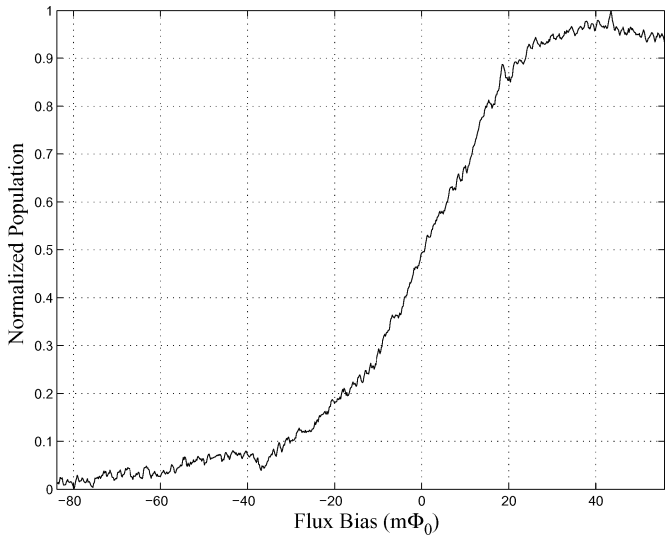

Fig. 2. A qubit step with the SQUID modulation curve subtracted. As the flux through the pc-qubit is swept from below to above one half flux quantum the system switches from being localized in the '0' state to the '1' state.

The ratio of the areas of the dc-SQUID and the pc-qubit were designed such that a qubit undergoes a transition for each 1.5 lobes of the SQUID modulation curve. The qubit signal is shown in Fig. 2 with the dc-SQUID modulation curve subtracted. The qubit modulated the dc-SQUID critical current by 100–300 nA, depending on its location along the SQUID modulation curve. The measurements were performed in a He^3 refrigerator with a base temperature of 350 mK. The electrical leads addressing the dc-SQUID were filtered with an RC filtering stage thermally anchored to the 1 K pot, and a stage of Cu powder filtering thermally anchored to the He^3 pot. Magnetic flux was supplied to the qubit-SQUID system from a coil external to the refrigerator, and the entire experiment was contained within a μ-metal insulating shield. Current was ramped to the SQUID linearly at 10 $\mu\mathrm{A}/\mathrm{ms}$, and the time was measured between the start of the current ramp and the switch of the dc-SQUID from the superconducting state the voltage state. The rate of the current ramp with the result of this measurement determines the switching current of the dc-SQUID, and hence can be used to measure the state of the qubit. The structure in the qubit step in Fig. 2 indicates evidence of incoherent tunneling between energy levels as the measurement SQUID is ramped. Rather than a smooth transition between the two states of the qubit as the flux is swept through $\Phi_0/2$, plateaus appear in the transition. This structure is due to excitations occurring at energy level anti-crossings caused by the mutual inductance between measurement SQUID and pc-qubit as the current to the SQUID is swept to make a measurement. The location of these anti-crossings can be mapped to an energy level bandstructure diagram. By fitting the bandstructure to the location of these plateaus the size of the qubit junctions can be determined [5]. Assuming that the junction undercut is equal for all three junctions in the pc-qubit loop, the sizes of the junctions were determined to be $0.4 \times 0.4\ \mu$m for the smaller junction and $0.5 \times 0.5\ \mu$m for the larger two, yielding $\alpha = 0.64$.

B. SQUID Oscillator

The dc-SQUID oscillator serves as a microwave source with tunable frequency and was designed to be highly overdamped $(\beta_c \ll 1)$ to allow for precise frequency adjustments of the device. The shunt resistors of the device (R_{sh}) were each 0.11 Ω, and the SQUID oscillator junctions were $\sim 120\ \mu\mathrm{m}^2$, yielding a critical current of ∼1.30 mA. The current-voltage characteristics when the oscillator is current biased above its critical current follow,

$$V_{osc}(I_{osc}) = I_{osc}R_{sh}\sqrt{1-\left(\frac{I_c^{osc}}{I_{osc}}\right)^2}, \qquad (1)$$

where V_{osc} is the time averaged voltage of the oscillator, I_{osc} is the external current supplied to the oscillator and I_c^{osc} is the critical current of the oscillator. Biased in the voltage state, the oscillator produces microwave radiation with a frequency governed by the Josephson relation, $f_{osc} = 2eV_{osc}/h$, where e is the electronic charge and h is Planck's constant.

The tank circuit coupled to the dc-SQUID oscillator serves as a bandpass filter suppressing unwanted harmonics produced by the Josephson oscillator which is highly nonlinear when operating at frequencies well below the plasma frequency (ω_p). The filter resistor (R_f), capacitor (C_f) and inductor (L_f) were designed to be 0.73 Ω, 4.6 pF and 75 pH, respectively. These values were not directly measured. The design is intended to couple flux, produced by currents oscillating in L_f, to the pc-qubit. The bandpass region for the oscillator-filter system is between approximately 7 to 11 GHz. The inductive loop of the dc-SQUID oscillator was designed such that mutual inductance between the oscillator and pc-qubit is zero, henceforth an external field modulating the pc-qubit has no effect on the oscillator and vice versa.

A critical concern when coupling to a quantum coherent system is the amount of decoherence that will be induced by the external system. The coherence time of the qubit must be longer than the time necessary to perform a coherent operation. The function of the oscillator is to couple coherent radiation to the qubit at the qubit splitting frequency, thereby driving coherent transitions between energy levels. For this to occur efficiently there must be a low impedance channel for current at this frequency, thereby creating an open channel for noise at this sensitive frequency. With this requirement in mind care has been taken to maximize amplitude of the current oscillations coupled to the qubit while minimizing the channel for decoherence by selection of the value of R_f. According to the spin-boson model of qubit decoherence, the decoherence rate of the qubit is proportional to the effective impedance of the environment to which the qubit is exposed. By choosing R_f appropriately the amplitude of the oscillations coupled to the qubit can be made large enough so that the qubit can be driven between energy levels more rapidly than the decoherence induced by the oscillator. See [6] for details.

III. Qubit—Oscillator Interaction

The experimental investigation of the interaction between the oscillator and qubit-SQUID system was conducted by repeatedly measuring the qubit step while incrementally increasing the current bias supplied to the oscillator. While the operating temperature of the experiment is sufficient to identify the qubit step and structure therein, it is too thermally energetic to obtain single-shot readout with the measurement scheme. Therefore, the statistical nature of the data requires that we examine trends in the statistics of the data as well as the data itself. Analysis of the qubit-oscillator interaction entailed examining the standard deviation of the data obtained when measuring the qubit step at each oscillator bias, and is shown in Fig. 3. The data indicate phenomena arising from the qubit—oscillator interaction that is dependent on the current bias to the oscillator and therefore dependent on the oscillator frequency. As the current bias to the oscillator is increased a peak arises in the standard deviation data and moves away from the center of the qubit step as the oscillator frequency is increased. As $\mathrm{I_{osc}}$ is increased above ∼1.37 mA the critical current of the measurement SQUID is suppressed along the entire region of the qubit step and the standard deviation increases accordingly, though in Fig. 3, the peak in the standard deviation is still apparent and maintains the trend followed in the rest of the data.

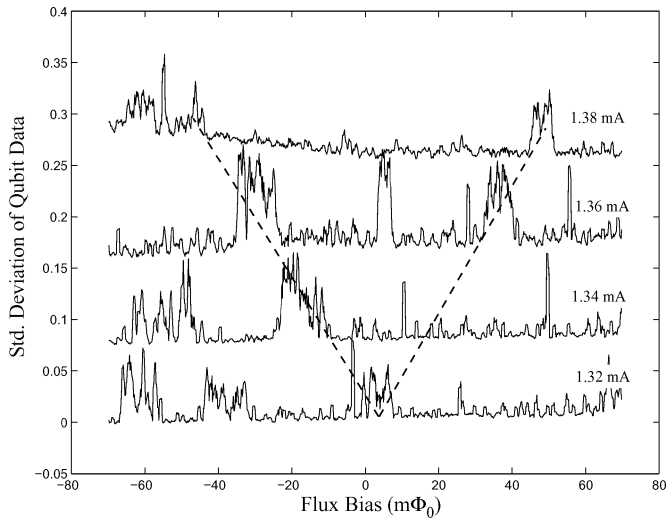

Fig. 3. This contour plots the standard deviation of the data from the qubit step as a function of I_{osc}. Horizontal slices are the data from the individual qubit steps. The data shows an increase in the standard deviation that moves away from the center of the step with increasing oscillator bias. When I_{osc} reaches 1.38 mA the signal from the measurement SQUID is suppressed by the oscillator.

Determining the frequency of the radiation produced by the oscillator from (1), the peaks appear to move away from the center of the qubit step at a rate $0.23\ \mathrm{GHz/m\Phi_0}$. By examining the bandstructure diagram that was calculated above, the trend in the standard deviation does not match an oscillator induced transition between the ground state and first excited state of the qubit, which has a slope $\sim 5.75\ \mathrm{GHz/m\Phi_0}$ as flux is modulated from the center of the qubit step. However, the data may match transitions between excited states that could be responsible for an increased tunneling rate and the subsequent rise in the standard deviation data. More conclusive results can be obtained by further removal of thermal energy by conducting experiments on the circuit in a dilution refrigerator.

IV. Conclusion

The data obtained from oscillator—qubit interaction indicate weak spectroscopic evidence and increased thermalization of the pc-qubit. Though operation at dilution refrigerator temperatures will reveal more striking quantum signatures, it is maintained that this type of on-chip oscillator represents the most rudimentary of the Josephson oscillator family, and was chosen for robust operation as opposed to optimal performance.

The oscillation stability of a highly damped Josephson junction has been thoroughly examined. The expression for the linewidth of a Josephson oscillator using the RSJ model is,

$$\Gamma = \pi \left(\frac{R_d^2}{R_N}\right) \left(\frac{2e}{\hbar}\right)^2 k_B T, \tag{2}$$

where k_B is Boltzmann's constant and T is temperature [7]. The dynamic resistance R_d is calculated by differentiating (1) with respect to I_{osc} and evaluating for $(I_{osc} > I_c^{osc})$. Using (2) and the parameters for our fabricated oscillator at 350 mK the oscillator linewidth is calculated to be 100 MHz at 10 GHz, a frequency typical for superconducting qubit operations. A linewidth of this order of magnitude is far larger than that from a room temperature microwave source and insufficient for performing quantum coherent manipulations of a superconducting qubit. Experimental measurements of simple Josephson oscillators, similar to ours, have been made [8] and the measured linewidths agree well with (2).

A great deal of effort has been focused on narrowing the linewidth and improving the phase stability of Josephson oscillators. Various types of Josephson oscillators exist, from long Josephson Junction resonant soliton [9] and flux-flow oscillators [10] to digital RSFQ ring oscillators [11], that can provide linewidths in the kHz range for performing qubit operations. External and on-chip phase locking techniques also exist to improve oscillator stability. Moreover, digital circuits can be used to provide quick pulses of radiation to the qubit, controlling their duration and periodicity [12].

Integrating already mature superconducting classical electronics with superconducting quantum bits will capitalize on the relative ease of scalability of superconducting quantum computer architectures over other implementations. Experiments like the one reported here must be increased in complexity and characterized in order to find efficient means for on-chip quantum control of superconducting qubits.

Acknowledgment

The authors would like to thank W. D. Oliver and J. C. Lee for valuable discussion and technical input. The authors would also like to thank K. K. Berggren and MIT Lincoln Laboratory for providing devices with which these experiments were conducted.

During the completion of this work, colleague and friend, B. Singh, passed away. His intellect and friendship will be missed.

References

[1] M. F. Bocko, A. M. Herr, and M. J. Feldman, "Prospects for quantum coherent computation using superconducting electronics," *IEEE Trans. Appl. Supercond.*, vol. 7, pp. 3638–3641, Jun. 1997.

[2] M. J. Feldman and M. F. Bocko, "A realistic experiment to demonstrate macroscopic quantum coherence," *Physica C*, vol. 350, no. 3–4, pp. 171–176, Feb. 2001.

[3] Y. Yu, D. Nakada, J. C. Lee, B. Singh, D. S. Crankshaw, T. P. Orlando, K. K. Berggren, and W. D. Oliver, "Energy relaxation time between macroscopic quantum levels in a superconducting persistent-current qubit," *Phys. Rev. Lett.*, vol. 92, no. 3, p. 117 904, Mar. 2004.

[4] I. Chiorescu, Y. Nakmura, C. J. P. M. Harmans, and J. E. Mooij, "Coherent quantum dynamics of a superconducting flux qubit," *Science*, vol. 299, no. 5614, pp. 1869–1871, Mar. 2003.

[5] D. S. Crankshaw, K. Segall, D. Nakada, T. P. Orlando, L. S. Levitov, S. Lloyd, S. O. Valenzuela, N. Markovic, M. Tinkham, and K. K. Berggren, "dc measurements of macroscopic quantum levels in a superconducting qubit structure with a time-ordered meter," *Phys. Rev. B*, vol. 69, no. 14, p. 144 518, Apr. 2004.

[6] D. S. Crankshaw, "Measurement and On-Chip Control of a Niobium Persistent Current Qubit," Ph.D. dissertation, Dept. of EECS, M.I.T, Cambridge, MA, 2003.

[7] K. K. Likharev, *Dynamics of Josephson Junctions and Circuits*. Philadelphia: Gordon and Breach, 1991, ch. 4.

[8] N. B. Dubash, Y. Zhang, U. Ghoshal, and P. Yuh, "Linewidth measurements and phase locking of Josephson oscillators using RSFQ circuits," *IEEE Trans. Appl. Supercond.*, vol. 7, pp. 3808–3811, Sep. 1997.

[9] J. L. Habif, C. A. Mancini, and M. F. Bocko, "Measurement of jitter in a long Josephson junction soliton oscillator clock source," *IEEE Trans. Appl. Supercond.*, vol. 11, pp. 1086–1089, Mar. 2001.

[10] V. P. Koshelets, P. N. Dmitriev, A. B. Ermakov, A. S. Sobolev, A. M. Baryshev, P. R. Wesselius, and J. Mygind, "Radiation linewidth of flux-flow oscillators," *Supercond. Sci. Technol.*, vol. 14, pp. 1040–1043, 2001.

[11] C. A. Mancini and M. F. Bocko, "Short-term frequency stability of clock generators for multigigahertz rapid-single-flux quantum digital circuits," *IEEE Trans. Appl. Supercond.*, vol. 13, pp. 25–37, Mar. 2003.

[12] D. S. Crankshaw, J. L. Habif, X. Zhou, T. P. Orlando, M. J. Feldman, and M. F. Bocko, "An RSFQ variable duty cycle oscillator for driving a superconducting qubit," *IEEE Trans. Appl. Supercond.*, vol. 13, pp. 966–969, Jun. 2003.